Hindawi
Advances in Civil Engineering
Volume 2022, Article ID 5630208, 17 pages
https://doi.org/10.1155/2022/5630208

Research Article

Optimal Design of Damped Structure with Inerter System Based on Modified Harmony Search Algorithm

Chao Pan,[1,2] **Xiao Han**,[2] **Hao Wang**,[1] **Dengke Yang**,[2] **and Li Zhang**[3]

[1]*State Key Laboratory of Mechanical Behavior and System Safety of Traffic Engineering Structures, Shijiazhuang Tiedao University, Shijiazhuang 050043, China*
[2]*College of Civil Engineering, Yantai University, Yantai 264005, China*
[3]*Department of Disaster Mitigation for Structures, Tongji University, Shanghai 200092, China*

Correspondence should be addressed to Hao Wang; wanghao@stdu.edu.cn

Received 17 January 2022; Revised 22 June 2022; Accepted 28 June 2022; Published 1 August 2022

Academic Editor: Agathoklis Giaralis

Copyright © 2022 Chao Pan et al. This is an open access article distributed under the Creative Commons Attribution License, which permits unrestricted use, distribution, and reproduction in any medium, provided the original work is properly cited.

An inerter system can amplify the deformation of its internal energy dissipation device, thereby improving the efficiency of energy dissipation and shock absorption. This is the so-called damping enhancement mechanism, one of the key mechanisms of the inerter system. Although the theoretical framework for damping enhancement of inerter systems has been established, the implementation of this principle for the design of an inerter system requires solving a complicated constrained optimization problem, which is not easy to be figured out using traditional approaches. To obtain valid design results through a lucid and robust method, it is proposed to optimize the damping parameters through a metaheuristic algorithm named harmony search algorithm in order to maximize the damping enhancement degree of the inerter system with the satisfaction of structural performance. First, the closed-form seismic response solutions of a single-degree-of-freedom (SDOF) structure with an inerter system are derived based on the theory of random vibration. Then, the mathematical expression of the constrained optimization problem is established. Due to the inefficiency of the original harmony search algorithm to solve the constrained optimization problem, the algorithm is modified by introducing a new harmony generating method and an adaptive strategy for parameter adjustment. The modified harmony search algorithm is compiled to solve the optimal design problem of the inerter system. The algorithm is verified by designing a structure with an inerter system. It is found that the number of iterations and time consumption until convergence required by the modified harmony search algorithm can be reduced by about 20%~90% compared with the original algorithm, which confirms the effectiveness of the modified algorithm. The results of dynamic analyses show that the structure have achieved the preset performance demands under different cases and the damping enhancement characteristic of the inerter system is fully utilized.

1. Introduction

The earthquake has become one of the main natural disasters that threaten the safety of human life and property because of its huge destructiveness. The destruction of engineering structures is the critical cause of earthquake disaster. Numerous studies have shown that structure control technology [1, 2] involving adding damping devices to the structure is an effective means to mitigate the structural response under earthquakes or strong winds or any other hazard that can cause vibration [3–5]. Inerter, a newly developed two-terminal acceleration-related element for structure control, can adjust the vibration characteristics of the structure flexibly and efficiently as its dynamic mass can reach thousands of times the physical mass [6, 7]. The realization mechanism of the inerter includes ball screw [8], rack-and-pinion [9], hydraulic [10], and electromagnetic mechanisms [11, 12]. The inerter system that is composed of an inerter, a spring, and an energy dissipation element (EDE; such as viscous, eddy current, magnetorheological dampers, etc.) has become an emerging shock absorption device with the excellent characteristic of damping enhancement. There are three typical types of inerter systems [13, 14]: series-layout inerter systems (SIS), series-parallel-layout type I

inerter systems (SPIS-I, also known as TID), and series-parallel-layout type II inerter systems (SPIS-II, also known as TVMD), which can be used in different cases to meet various demands for structure control.

The research team headed by Inoue and Ikago et al. from Tohoku University firstly proposed the inerter system (termed tuned viscous mass damper, TVMD for short) at the end of the last century. Ikago et al. [6] derived the formulae for estimating parameters of TVMD in a single-degree-of-freedom (SDOF) structure based on the fixed-point theory, which has become the classical design method for the inerter system. Subsequently, analogous to the tuned mass damper (TMD), Lazar et al. [15] proposed a tuned inerter damper (TID) and proved that the TIDs installed between adjacent floors of multistorey buildings can preferably amplify the damping effect compared with traditional TMDs. Afterward, many scholars studied the further characteristics of the TID. Among them, Gonzalez-Buelga et al. [16] studied the nonlinear characteristics of TID and conducted real-time hybrid simulation experiments. De Domenico et al. [17, 18] attached TID to the base isolation layer for optimized design. With the continuous deepening of research, Marian et al. [19] proposed a tuned mass damping inertial (TMDI) container, which is characterized by installing an inerter in the TMD system. They found that the TMDI is better than the classic TMD in reducing the displacement response. Pietrosanti et al. [20] optimized the SDOF structure by minimizing structural displacement and acceleration under white noise excitation and maximizing the ratio of TMDI energy consumption to total input energy. Park and Giarails et al. [21] pointed out that TMDI can reduce the additional mass and more effectively control the acceleration responses compared with traditional TMD. De Domenico and Ricciardi [22] applied TMDI to a base isolation structure to effectively reduce the displacement of the isolation layer, the bottom shear force, and the displacement angle of the upper structure. Jin et al. [23] comparatively studied the two connection forms of TMDI and analyzed the influence of the mass ratio of the tuned mass damper and the inertance-mass ratio on the performance of the system. Zhang et al. [24] proposed the strategy of using a distributed tuned inerter system to control the seismic response in multiple modes in the high-rise chimney, which achieved the lightweight effect. Faraj et al. [25] proposed a new method to adjust the inertial mass of the inerter by using impact energy management to absorb impact and store it in a special device. Javidialesaadi and Wierschem [26] proposed a new type of nonlinear energy absorber equipped with an inerter system for passive vibration control of structures. Zhao et al. [27, 28] proposed an equation from the perspective of energy, which produces an analysis method for evaluating the input power of an inerter-based structure and quantifying the energy dissipation effect of the inerter system. Pan and Zhang et al. [29–31] proposed principles and methods for the optimal design of inerter system considering structural performance demand and control cost simultaneously based on random vibration theory. Subsequently, Zhang and Pan et al. [32–34] discovered the principle of damping enhancement of the inerter system based on the analytical solution of the random vibration response, and the principle can provide a clear physical explanation of the mechanism of the inerter system.

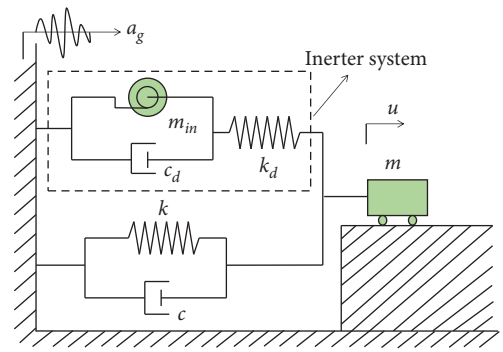

Figure 1: Mechanical model of an SDOF system with the inerter system.

Damping enhancement, a mechanism of inerter system with clear physical meanings, has been adopted as the optimal design principle for a structure with an inerter system. However, traditional numerical optimization methods require complicated gradient expressions and appropriate initial guesses, which are not easy to obtain. Gradient metaheuristic algorithms provide an alternative way to perform optimization in engineering practice [35–39]. Although new algorithms emerge one after another nowadays, such as grey wolf optimizer [40], chaos game optimization [41], aquila optimizer [42], and atomic orbital search [43], the classical algorithms are still vital because they are simple, easy to implement, well-known, and widely accepted. The harmony search algorithm is just one of the widely used classical algorithms in the field of structural control. Bekda and Nigdeli [44] proposed using harmony search algorithm to find the best parameters for tuned mass dampers. Yazdi et al. [45] proposed an improved harmony search algorithm for designing tuned mass dampers, and it is found that the improved harmony search algorithm is more efficient than the gene algorithm and the particle swarm optimization algorithm. Nigdeli and Alhan [46] optimized the parameters of the seismic isolation system through the harmony search algorithm. Ocak et al. [47] optimized TLDs via metaheuristic methods, including the harmony search algorithm. Ulusoy et al. [48] used the harmony search algorithm to investigate the PID parameters of a multistorey structure incorporating active tendon control systems. These studies show the good performance of the harmony search algorithm and provide a theoretical basis for this paper.

To perform the optimization of the inerter system, one of the novel structural control systems, more efficiently and robustly, a modified harmony search algorithm with better performance is proposed in this study. First, the closed-form stochastic seismic response solutions of an SDOF structure with an inerter system are derived based on the theory of random vibration under white-noise excitation, and then the mathematical description of the damping enhancement maximization principle of the inerter system is provided. To obtain the solutions more efficiently, a new harmony generation method is proposed as an improvement to the original harmony search algorithm. Besides, an adaptive

Table 1: Notations.

Notation	Definition
$p(t)$	External excitation
a_g	Acceleration of ground motion
m	Mass of the primary SDOF structure
c	Damping coefficient of the primary SDOF structure
k	Stiffness of the primary SDOF structure
u	Displacement response of the primary SDOF structure
$\dot{u}$	Velocity response of the primary SDOF structure
$\ddot{u}$	Acceleration response of the primary SDOF structure
F_{IS}	The control force of the inerter element
k_d	Stiffness of the spring element in the inerter system
c_d	Damping coefficient of the EDE in the inerter system
m_{in}	Inertance of the inerter
u_{in}	Displacement response of the inerter
$\dot{u}_{in}$	Velocity response of the inerter
$\ddot{u}_{in}$	Acceleration response of the inerter
$\omega_0 = \sqrt{k/m}$	Original circular frequency of the primary SDOF structure
$\zeta = c/2m\omega$	Inherent damping ratio of the primary SDOF structure
$\mu = m_{in}/m$	Inertance-mass ratio of the inerter system
$k = k_d/k$	Stiffness ratio of the inerter system
$\xi = c_d/2m\omega$	Nominal damping ratio of the inerter system
U	Laplace transformation of u
$H_U(i\omega)$	The frequency-domain transfer function of u
A_g	Laplace transformation of a_g
S_0	The amplitude of the input power spectral density of white-noise excitation
σ_u^2	Stochastic mean square deformation response of the structure
$\sigma_{u,d}^2$	Stochastic mean square deformation response of the EDE in the inerter system
$\sigma_{u,0}^2$	Stochastic mean square displacement response of the original SDOF structure
γ	Stochastic response mitigation ratio
α	Damping deformation enhancement factor (DDEF)
u_d	Deformation of the EDE in the inerter system
γ_t	Target response mitigation ratio according to performance demands
ω	Circular frequency of harmonic excitation
$\beta = \omega/\omega_0$	Relative frequency of harmonic excitation
HM	Harmony memory
$HMCR$	Harmony memory considering rate
PAR	Pitch adjusting rate
HMS	Harmony memory size

adjustment strategy of the parameters in harmony search algorithm is adopted to improve the solving efficiency further. Then a computer program is developed to solve the nonlinear constraint optimization problem of the inerter system by the modified harmony search algorithm. Finally, the design cases are executed to prove the effectiveness of the proposed algorithm compared with the original algorithm and an existing harmony search algorithm. Meanwhile, the structural dynamic analysis of the design cases shows that the designed parameters have met the preset performance demands and the damping enhancement characteristics of the inerter system are fully utilized. Moreover, what needs to be pointed out is that the focus of the paper is the modification of the harmony search algorithm, so that only the simple SDOF structure is concerned in this paper. In fact, optimized parameters obtained from an SDOF structure can also be used in a multi-degree-of-freedom structure through certain mathematical transformations [31]. That is to say, the research works on an SDOF structure with an inerter system are meaningful.

2. Theoretical Basis of Structure with the Inerter System

2.1. Equation of Motion for SDOF Structure with the Inerter System. When an SDOF structure with an inerter system (as shown in Figure 1) is subjected to a ground motion excitation (the acceleration of the ground motion is a_g), the equation of motion can be established as follows:

$$m\ddot{u} + c\dot{u} + ku + F_{IS} = -ma_g. \tag{1}$$

The corresponding extra equations with respect to F_{IS} are as follows:

$$\begin{cases} F_{IS} = k_d(u - u_{in}) \\ m_{in}\ddot{u}_{in} \end{cases} + c_d\dot{u}_{in} = k_d(u - u_{in}). \tag{2}$$

The definitions of the other symbols can be found in Table 1.

Therefore, the integrated equation of motion for an SDOF system with the inerter system is

$$\left\{ m\ddot{u} + c\dot{u} + ku + k_d(u - u_{in}) = -ma_g m_{in}\ddot{u}_{in} + c_d\dot{u}_{in} = k_d(u - u_{in}). \right. \tag{3}$$

2.2. Closed-Form Expressions of Stochastic Response. Both sides of equation (3) are divided by m to normalize as follows:

$$\left\{ \ddot{u} + 2\zeta\omega_0\dot{u} + \omega_0^2 u + \kappa\omega_0^2(u - u_{in}) = -a_g\mu\ddot{u}_{in} + 2\xi\omega_0\dot{u}_{in} = \kappa\omega_0^2(u - u_{in}). \right. \tag{4}$$

The definitions of key symbols in (4) are shown in Table 1. It can be found that $\mu, \xi, \text{and } \kappa$ are the three key parameters for the inerter system.

Equation (4) can be transformed into the Laplace domain, and then the displacement frequency-domain transfer function of the primary SDOF structure can be obtained as

$$H_U(s) = \frac{s^2\mu + 2s\xi\omega_0 + \kappa\omega_0^2}{\kappa^2\omega_0^4 - \left(s^2\mu + 2s\xi\omega_0 + \kappa\omega_0^2\right)\cdot\left[s^2 + 2s\zeta\omega_0 + (1+\kappa)\omega_0^2\right]}. \tag{5}$$

According to the random vibration theory [49], under the white-noise excitation (power spectral density is S_0), the mean square value of the structure displacement response is as follows:

$$\sigma^2 = \int_{-\infty}^{\infty} |H(i\omega)|^2 S_0 d\omega. \tag{6}$$

By substituting (5) into (6), the closed-form expression of the stochastic mean square value of the deformation response of the SDOF structure with inerter system can be obtained [28]:

$$\sigma_u^2 = \frac{\pi S_0}{2\omega_0^3}\cdot\frac{A}{B}, \tag{7}$$

$$\begin{aligned} A = {} & 4\zeta^2\kappa\mu\xi + \xi\left[\kappa^2 + \kappa(-2+\mu)\mu + \mu^2 + 4\xi^2\right] \\ & + \zeta\left(\kappa^2\mu^2 + 4\kappa\xi^2 + 4\mu\xi^2\right), \end{aligned} \tag{8}$$

$$\begin{aligned} B = {} & 4\zeta^3\kappa\mu\xi + \kappa^2\xi^2 + \zeta^2\left[\kappa^2\mu^2 + 4\mu\xi^2 + 4\kappa(1+\mu)\xi^2\right] \\ & + \zeta\xi\left[\mu^2 + \kappa^2\left(1+\mu^2\right) + 4\xi^2 + 2\kappa\left(-\mu + \mu^2 + 2\xi^2\right)\right]. \end{aligned} \tag{9}$$

The closed-form expression of stochastic mean square deformation response of the EDE in the inerter system is

$$\sigma_{u,\mathrm{d}}^2 = \frac{\pi S_0}{2\omega_0^3}\cdot\frac{\kappa\left[\zeta(1+\kappa)\mu^2 + \kappa\xi + 4\zeta^2\mu\xi + 4\zeta\xi^2\right]}{F}, \tag{10}$$

$$\begin{aligned} F = {} & 4\zeta^3\kappa\mu\xi + \kappa^2\xi^2 + \zeta^2\left[\kappa^2\mu^2 + 4\mu\xi^2 + 4\kappa(1+\mu)\xi^2\right] \\ & + \zeta\xi\left[\mu^2 + \kappa^2\left(1+\mu^2\right) + 4\xi^2 + 2\kappa\left(-\mu + \mu^2 + 2\xi^2\right)\right]. \end{aligned} \tag{11}$$

For a classic SDOF structure, the stochastic mean square deformation response can be expressed as follows:

$$\sigma_{u,0}^2 = \frac{\pi S_0}{2\omega_0^3}\cdot\frac{1}{\zeta}. \tag{12}$$

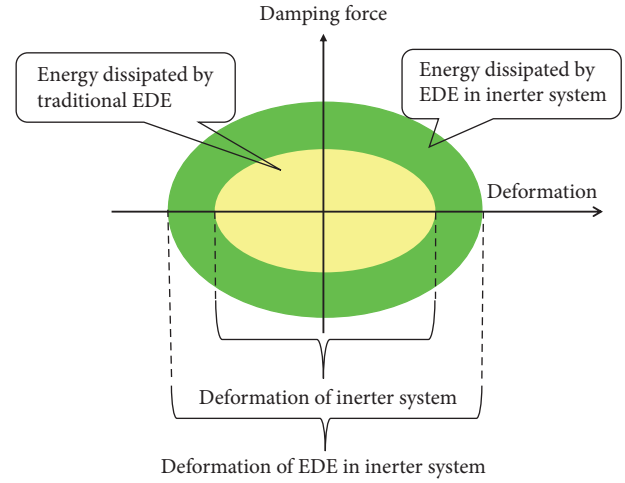

Figure 2: Damping enhancement of inerter system.

Table 2: Comparison of optimization and music performance.

Analogy element	Analogy diagram: Optimization process	Analogy diagram: Realization process
Best state	Global best	Excellent harmony
Be evaluated by...	Objective function	Aesthetic evaluation
Evaluate with...	Design variable value	Pitch of the instrument
Process unit	Every iteration	Every practice

Based on the random vibration response expression, the stochastic response mitigation ratio of the structures with inerter system γ can be defined as [29]

$$\begin{aligned} \gamma &= \frac{\text{response of structure with inerter system}}{\text{response of original structure}} \\ &= \sqrt{\frac{\sigma_u^2(\zeta,\mu,\xi,\kappa)}{\sigma_{u,0}^2(\zeta)}}. \end{aligned} \tag{13}$$

By substituting (7) and (12) into (13), the expression of the stochastic response mitigation ratio of the structure inerter system is as follows:

$$\begin{aligned} P = {} & 4\zeta^2\kappa\mu\xi + \xi\left[\kappa^2 + \kappa(-2+\mu)\mu + \mu^2 + 4\xi^2\right] \\ & + \zeta\left(\kappa^2\mu^2 + 4\kappa\xi^2 + 4\mu\xi^2\right) \\ Q = {} & 4\zeta^3\kappa\mu\xi + \kappa^2\xi^2 + \zeta^2\left[\kappa^2\mu^2 + 4\mu\xi^2 + 4\kappa(1+\mu)\xi^2\right] \\ & + \zeta\xi\left[\mu^2 + \kappa^2\left(1+\mu^2\right) + 4\xi^2 + 2\kappa\left(-\mu + \mu^2 + 2\xi^2\right)\right]. \end{aligned} \tag{14}$$

2.3. Optimization Problem of Structure with the Inerter System. When the inerter system resonates with the external excitation, the internal freedom of the inerter system has a phase difference with respect to the vibration of the primary

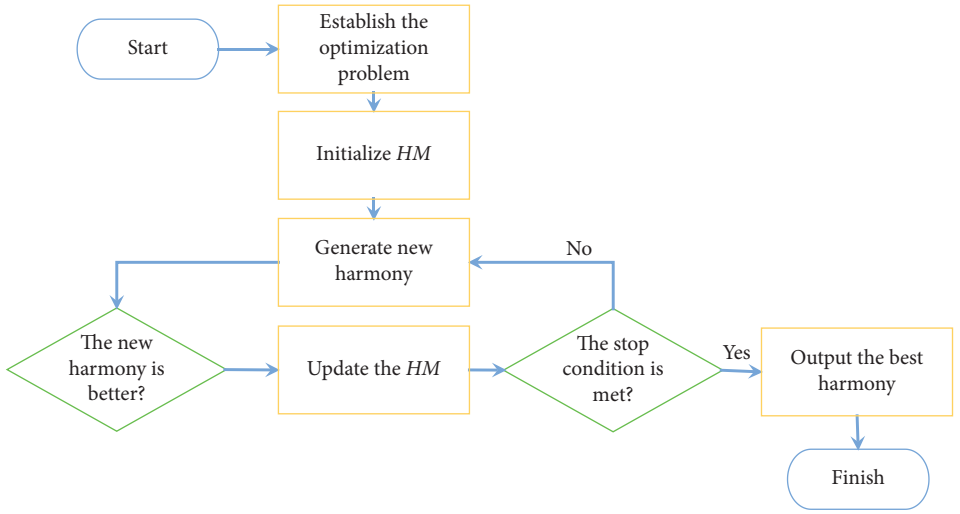

Figure 3: Flowchart of harmony search algorithm.

structure [32], so that the displacement of the internal freedom of the inerter system will be greater than its deformation of the primary structure. Therefore, the inerter system can absorb and dissipate more input energy compared with a directly installed traditional EDE and can reduce the dynamic response of the structure more efficiently, as shown in Figure 2.

To measure the degree of damping enhancement, Zhang et al. [32] defined a dimensionless parameter damping deformation enhancement factor (DDEF) α as follows:

$$\alpha = \frac{\text{deformation of EDE of the inerter system}}{\text{deformation of the inerter system}}. \tag{15}$$

Considering (7) and (10), the specific expression of DDEF for an inerter system in an SDOF structure is as follows:

$$\alpha = \sqrt{\frac{\kappa\left[\zeta(1+\kappa)\mu^2 + \kappa\xi + 4\zeta^2\mu\xi + 4\zeta\xi^2\right]}{4\zeta^2\kappa\mu\xi + \zeta\left(\kappa^2\mu^2 + 4\kappa\xi^2 + 4\mu\xi^2\right) + \xi\left[\kappa^2 + \kappa(\mu-2)\mu + \mu^2 + 4\xi^2\right]}}. \tag{16}$$

To give full play to the damping enhancement characteristics of the inerter system, the key parameters of the inerter system should be optimized based on the principle of maximizing the damping enhancement degree of the inerter system with satisfaction of structural performance. The above optimization problem can be expressed as a constrained optimization problem:

$$\begin{aligned} \max \quad & f(\mu,\xi,\kappa) = \alpha(\mu,\xi,\kappa) \\ \text{s.t.} \quad & \gamma(\mu,\xi,\kappa) = \gamma_t \\ & 0 \le \mu \le 1 \\ & 0 \le \xi \le 1 \\ & 0 \le \kappa \le 1. \end{aligned} \tag{17}$$

In (17), $f(\mu,\xi,\kappa) = \alpha(\mu,\xi,\kappa)$ is the objective function; γ_t is the target stochastic response mitigation ratio [29], according to the damping enhancement equation of the inerter system [32]:

$$\alpha^2 = \frac{\zeta}{\xi}\left(\frac{1}{\gamma^2} - 1\right). \tag{18}$$

When γ is constant, the DDEF of the inerter system is inversely proportional to its nominal damping ratio. In other words, when α reaches the maximum value, ξ would reach the minimum value. Therefore, the constrained optimization problem can be rewritten as follows:

$$\begin{aligned} \min \quad & f(\mu,\xi,\kappa) = \xi \\ \text{s.t.} \quad & \gamma(\mu,\xi,\kappa) = \gamma_t \\ & 0 \le \mu \le 1 \\ & 0 \le \xi \le 1 \\ & 0 \le \kappa \le 1. \end{aligned} \tag{19}$$

For the established constrained optimization problem, if the classical numerical calculation method is adopted, the calculation process is complicated due to the cumbersome mathematical expressions. In order to simplify the calculation, zero inherent damping is usually assumed for the primary SDOF structure, which is not accurate enough. As a metaheuristic algorithm, the harmony search algorithm has the advantages of simple principle, simple operation, easy implementation, and strong search diversity. By adopting the algorithm, it is not necessary to ignore the existence of the inherent damping ratio of the primary SDOF structure and is easy to adjust when the topological form of the inerter system or the structure is changed. Therefore, this paper chooses to modify the harmony search algorithm to optimize the key parameters of the structure with inerter system.

3. Harmony Search Algorithm and Modification

3.1. Original Algorithm. The harmony search algorithm is a novel intelligent optimization algorithm proposed by Z. W. Geem et al. in 2001. The harmony search algorithm simulates

Table 3: The three benchmark functions.

Function category	Function name	Function	Dim	Range	$f_{\min}$
Unimodal benchmark function	Sphere function	$f_1(x) = \sum_{i=1}^{n} x_i^2$	30	$[-100, 100]$	0
	Generalized Rosenbrock's function	$f_5(x) = \sum_{i=1}^{n-1} [100(x_{i+1} - x_i^2)^2 + (x_i - 1)^2]$	30	$[-30, 30]$	0
Multimodal benchmark function	Generalized Rastrigin's function	$f_9(x) = \sum_{i=1}^{n} [x_i^2 - 10\cos(2\pi x_i) + 10]$	30	$[-5.12, 5.12]$	0
Constrained minimization problem		$\min \quad f(x) = (x_1 - 2)^2 + (x_2 - 1)^2$ $s.t. \quad x_1 - 2x_2 + 1 = 0$ $\quad -x_1^2/4 - x_2^2 + 1 \geq 0$	2	$[0, 1]$	1.3935

Table 4: The average solution of benchmark functions.

Function category	Function	Average value of objective function		
		Original harmony search algorithm	Improved harmony search algorithm [45]	Modified harmony search algorithm
Unimodal benchmark function	f_1	5.075197	0.000154	0.000185
	f_5	1.796811	0.000017	0.078591
Multimodal benchmark function	f_9	3.440918	0.011626	0.032503
Constrained minimization problem		1.393897	1.389428	1.393615

the procedure of music creation. The musicians rely on their memory to understand the pitch of the instruments in the band. Repeated adjustments finally made the band play a beautiful harmony state. The analogy is shown in Table 2 [50].

The procedure of the original harmony search algorithm (Figure 3) can be summarized as follows.

Step 1. Establish the optimization problem (take solving the minimization problem as an example).

$$\min f(\vec{X}), \tag{20}$$

where $f(\vec{X})$ is the objective function to be optimized; $\vec{X} = (x_1, x_2, \cdots, x_i \cdots, x_n)$ is the solution vector and $x_i (i = 1, 2, \cdots, n)$ is the decision variable that constitutes the solution vector; n is the dimension of solution space.

Step 2. Initialize *HM*. Randomly generate *HMS* harmonies, and put them into *HM*; the mathematical form of *HM* is as follows:

$$HM = \begin{bmatrix} \vec{X}^{(1)} \\ \vec{X}^{(2)} \\ \vdots \\ \vec{X}^{(HMS)} \end{bmatrix} = \begin{bmatrix} x_1^{(1)} & x_2^{(1)} & \cdots & x_n^{(1)} \\ x_1^{(2)} & x_2^{(2)} & \cdots & x_n^{(2)} \\ \vdots & \vdots & \cdots & \vdots \\ x_1^{(HMS)} & x_2^{(HMS)} & \cdots & x_n^{(HMS)} \end{bmatrix}. \tag{21}$$

Step 3. Generate a new harmony. When a random number is greater than the retention probability *HMCR*, the new harmony is randomly generated in the feasible region. Otherwise, a new harmony is generated as follows:

$$\vec{x}_{new}(i) = HM(R, i), \tag{22}$$

where R is a random number between 1 and *HMS*.

For every tone in the new harmony, if a randomly generated random number is less than *PAR*, the tone is randomly generated near the original tone:

$$\vec{x}_{new} = \vec{x}_{new} + bw \cdot 2(\overrightarrow{Rand} - 0.5), \tag{23}$$

where bw is bandwidth for pitch adjusting; $\overrightarrow{Rand}$ is a vector that contains randomly generated values between 0 and 1.

Step 4. Update the *HM*. If the new harmony vector is better than the worst vector in the *HM*, then the new vector replaces

Table 5: Design optimization parameters of the structure with the inerter system based on the modified harmony search algorithm.

Case	Optimized parameters						
	ζ	γ_t	μ	ξ	κ	γ	α
1	0.02	0.70	0.0113	0.0004	0.0113	0.6981	7.25236
2	0.02	0.60	0.0282	0.0016	0.0289	0.5981	4.73649
3	0.02	0.50	0.0680	0.0061	0.0727	0.5005	3.13189
4	0.02	0.45	0.1058	0.0123	0.1176	0.4500	2.53163
5	0.05	0.70	0.0655	0.0053	0.0692	0.7000	3.1333
6	0.05	0.60	0.1437	0.0188	0.1648	0.5999	2.1750
7	0.05	0.50	0.2832	0.0581	0.3848	0.5000	1.60672
8	0.05	0.45	0.3800	0.0981	0.5949	0.4500	1.41687

Note. The inherent damping ratio ζ and the target response mitigation ratio γ_t are the performance indices.

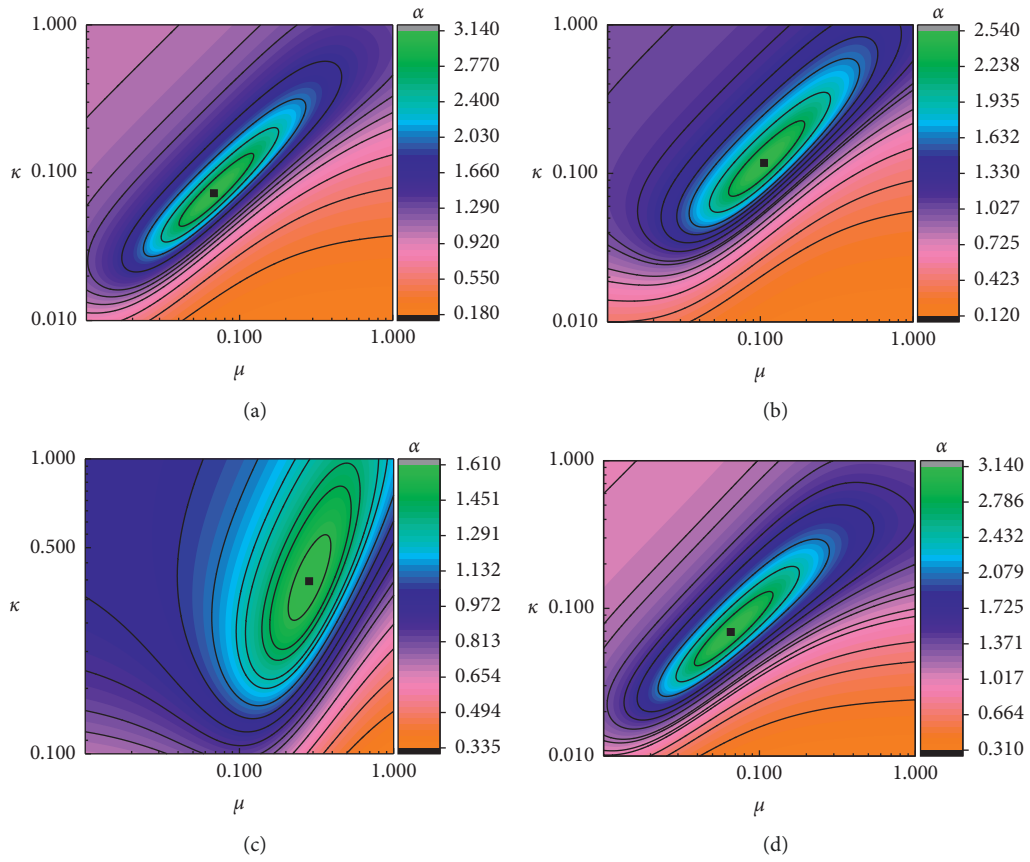

Figure 4: Contours of the damping deformation enhancement factor α of an SDOF structure with the inerter system (note: the black square in the figure represents the parameters optimized by the modified harmony search algorithm). (a) Case 3. (b) Case 4. (c) Case 7. (d) Case 5.

Table 6: Average convergent iterations of modified and original harmony search algorithms.

Case	Original harmony search algorithm			Modified harmony search algorithm			Rate of increase (%)	
	Number of iterations at the convergence	Number of the objective function evaluations	Consumed Time (s)	Number of iterations at the convergence	Number of the objective function evaluations	Consumed time (s)	Number of iterations at the convergence	Consumed time
1	>100000	301701	>7.21	29927	92432	3.04	>70.07	>57.86
2	>100000	304551	>7.28	13700	43251	1.36	>86.30	>81.83
3	>100000	306651	>7.32	7922	25917	0.81	>92.08	>88.91
4	52100	163601	3.81	19260	62331	1.90	63.03	50.00
5	>100000	304701	>7.64	9097	29392	0.86	>90.90	>88.74
6	27397	89342	2.01	16789	55868	1.64	38.72	18.47
7	39431	130344	2.86	20565	68246	1.99	47.85	30.39
8	42582	144897	3.12	22371	75014	2.28	47.46	26.80

Note. The symbol ">" indicates that, during the 100 solutions of the case, there are 1 or more nonconvergent solutions. The computer for calculation is a common office computer with an Intel Core i7-6700 CPU and an 8 GB RAM. Since the improved harmony search algorithm [45] did not converge in all solutions, the results are not listed here.

the worst harmony vector; otherwise, no operation is performed.

Step 5. Check whether the stop condition is reached; if the stop condition is reached, the algorithm terminates; otherwise, the algorithm repeats steps 3-4.

3.2. Modification of Harmony Search Algorithm. With the widespread application of the harmony search algorithm, scholars continue to develop some modifications over the original harmony search algorithm. For example, Omran and Mahdavi [51] improved the search mechanism of harmony and proposed a global harmony search. Fesangharya et al. [52] proposed a hybrid harmony search algorithm and so on.

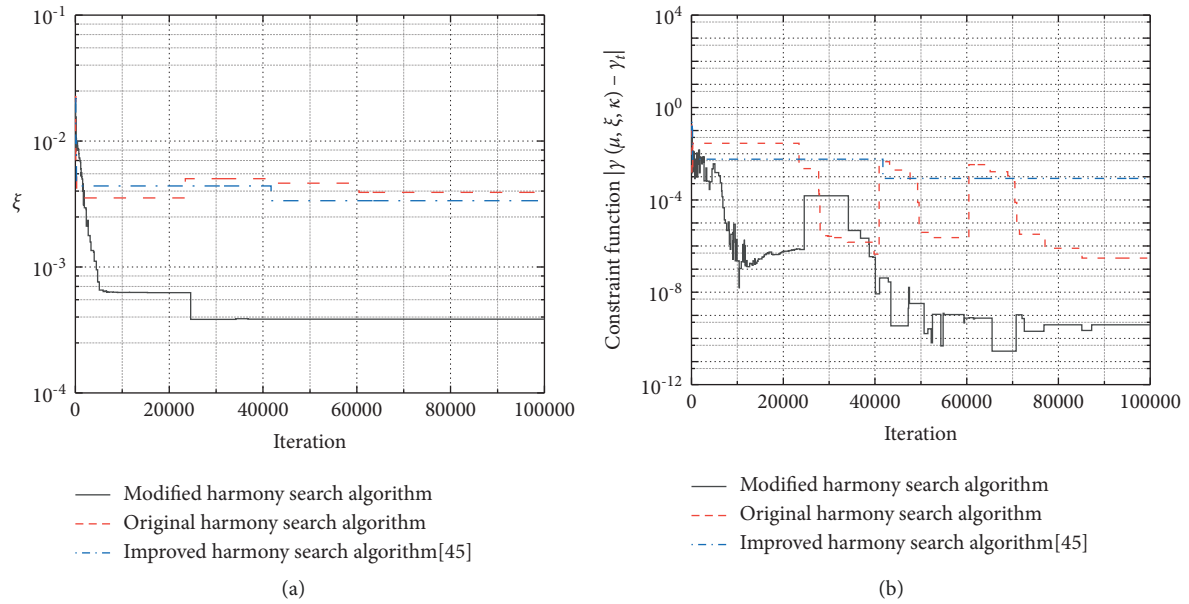

Figure 5: The variation trends of key indices during the optimization process for case 1. (a) The nominal damping ratio ξ. (b) The constraint function $|\gamma(\mu, \xi, \kappa) - \gamma_t|$.

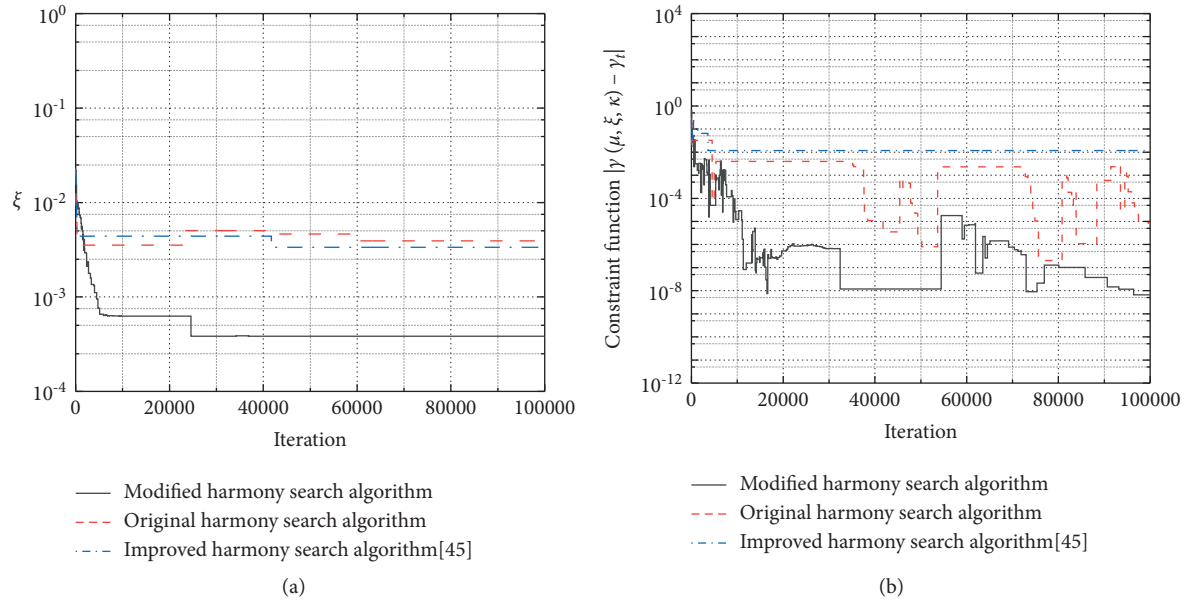

Figure 6: The variation trends of key indices during the optimization process for case 2. (a) The nominal damping ratio ξ. (b) The constraint function $|\gamma(\mu, \xi, \kappa) - \gamma_t|$.

The original harmony search algorithm is not efficient for solving constrained optimization problems. Given this, a simple modification is made to replace the classic behavior of generating new harmony in this paper, that is, select two harmonies $\vec{x}_i, \vec{x}_j$ in the *HM* and generate a new harmony as follows:

$$\vec{x}_{new} = \vec{x}_i + 2(\overrightarrow{Rand} - 0.5)\left(\vec{x}_j - \vec{x}_i\right). \tag{24}$$

In (24), $\overrightarrow{Rand}$ is a random vector, and each value of it is between 0 and 1. The selection of the harmonies $\vec{x}_i, \vec{x}_j$ is based on the individual fitness value f_i and the cumulative probability p_i, which are calculated as follows:

$$p_i = \sum_{k=1}^{i} f_k / \sum_{k=1}^{n} f_k. \tag{25}$$

If a generated random number is greater than p_{i-1} and less than p_i, the i-th harmony is selected.

PAR and *bw* play an important role in searching for high-quality harmony. To carry out an effective search in the

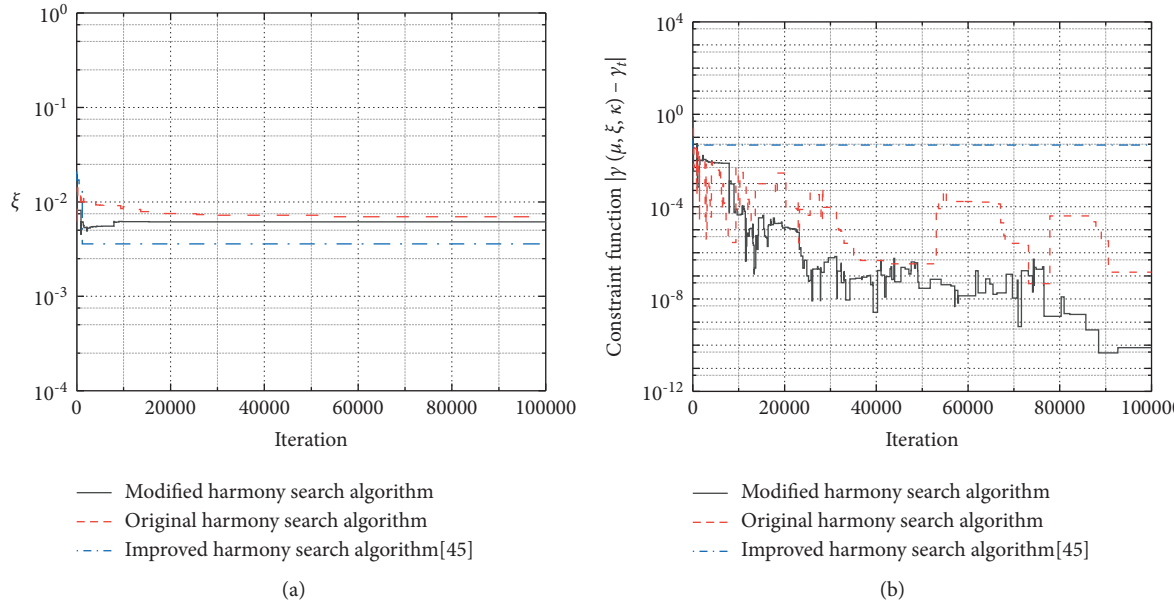

Figure 7: The variation trends of key indices during the optimization process for case 3. (a) The nominal damping ratio ξ. (b) The constraint function $|\gamma(\mu, \xi, \kappa) - \gamma_t|$.

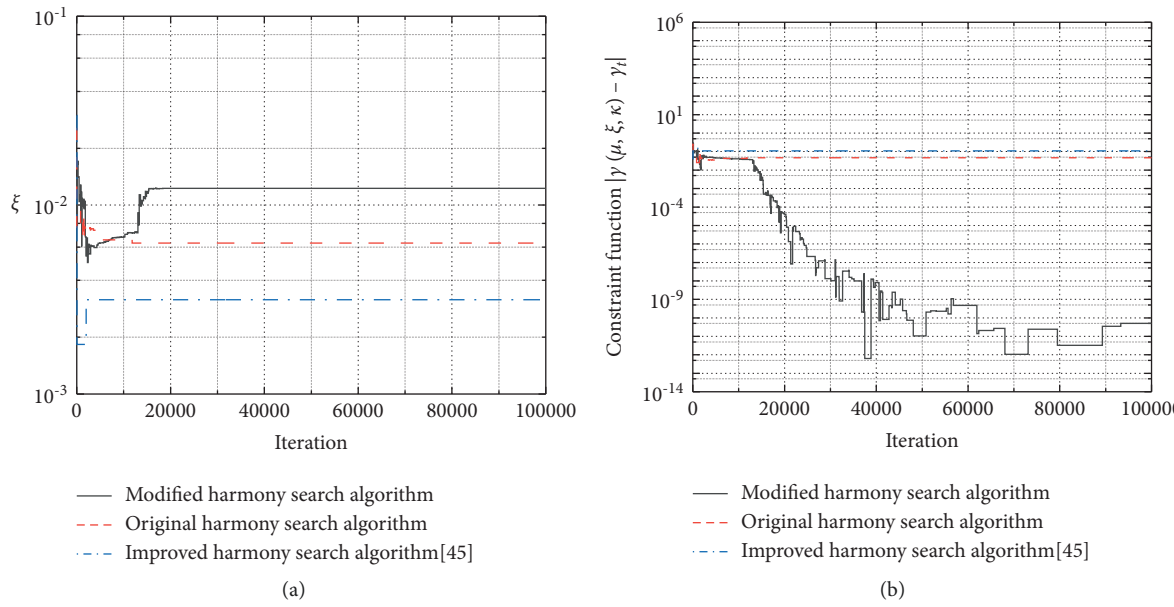

Figure 8: The variation trends of key indices during the optimization process for case 4. (a) The nominal damping ratio ξ. (b) The constraint function $|\gamma(\mu, \xi, \kappa) - \gamma_t|$.

whole solution space and improve the efficiency of the algorithm, PAR and bw are set to change adaptively as follows [53]:

$$PAR = PAR_{\min} + \frac{PAR_{\max} - PAR_{\min}}{N_{iter}} \cdot t, \tag{26}$$

$$bw = bw_{\max} \cdot e^{\frac{t}{N_{iter}} \log \frac{bw_{\min}}{bw_{\max}}}. \tag{27}$$

The damping enhancement optimization problem of the inerter system is a constrained optimization problem, and the modified harmony search algorithm is essentially an unconstrained search method. Therefore, the penalty function method is adopted to convert the optimization problem of the inerter system into an unconstrained optimization problem, so that the modified harmony search algorithm can be applied. After introducing the penalty function, the expression of the optimization problem of the inerter system is as follows:

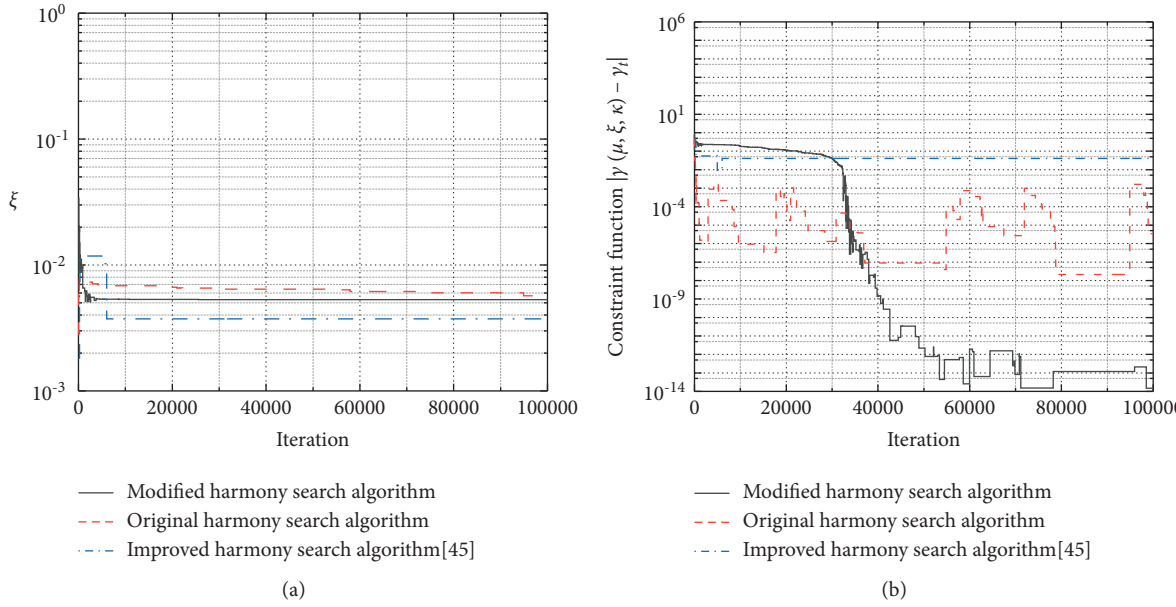

Figure 9: The variation trends of key indices during the optimization process for case 5. (a) The nominal damping ratio ξ. (b) The constraint function $|\gamma(\mu, \xi, \kappa) - \gamma_t|$.

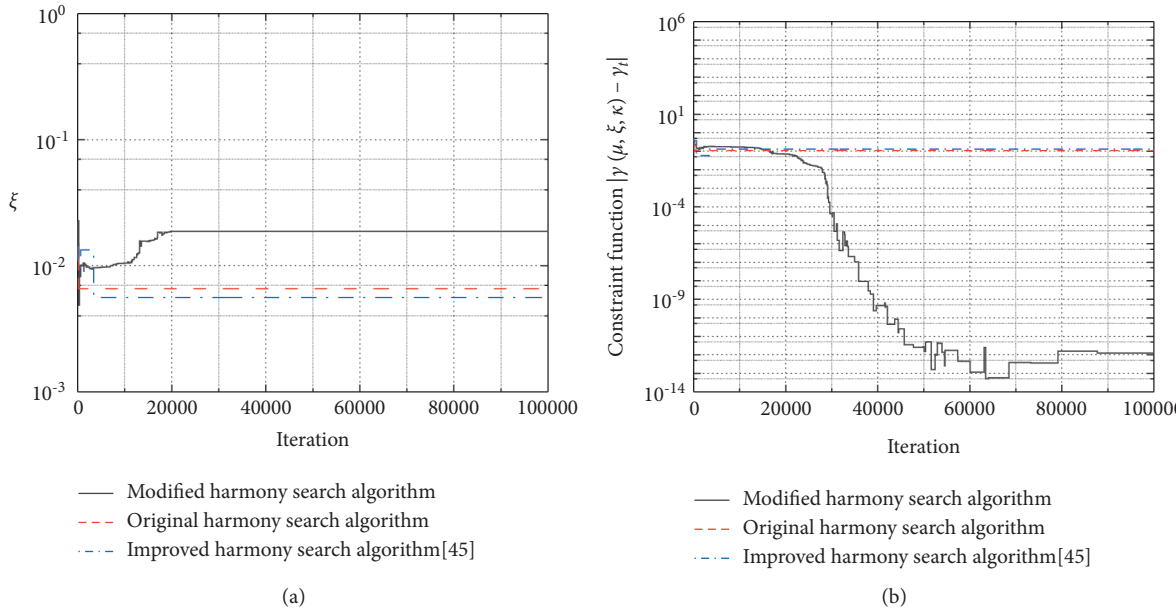

Figure 10: The variation trends of key indices during the optimization process for case 6. (a) The nominal damping ratio ξ. (b) The constraint function $|\gamma(\mu, \xi, \kappa) - \gamma_t|$.

$$\underset{\mu,\xi,\kappa\in[0,1]}{\text{minimize}} \quad f(\mu, \xi, \kappa) = \xi + h \cdot \left|\gamma(\mu, \xi, \kappa) - \gamma_t\right|, \tag{28}$$

where h is the penalty factor that can eliminate individuals who do not meet the constraint. However, a proper penalty factor is not easy to be found to obtain a satisfactory solution. Given this, an adaptive penalty factor is adopted in this paper, and its expression is

$$h = h_0 \cdot \delta^{t_s}. \tag{29}$$

In (29), δ and h_0 are constants, and their value ranges are suggested to be $\delta \in (1, 1.1)$ and $h_0 \in (0.01, 0.1)$; t_s is the

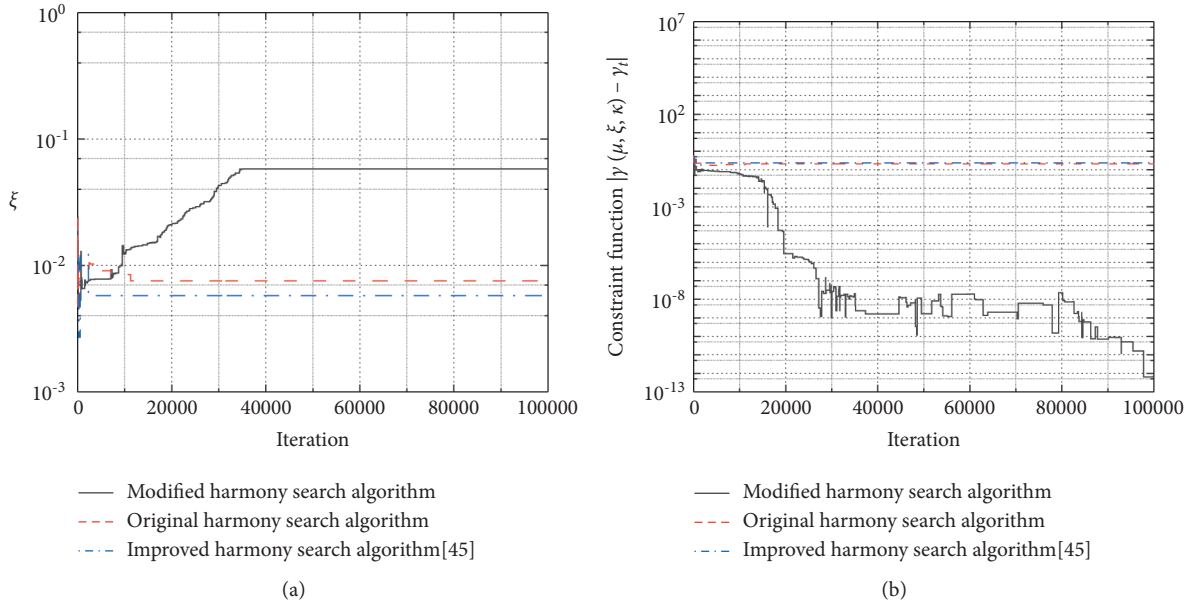

Figure 11: The variation trends of key indices during the optimization process for case 7. (a) The nominal damping ratio ξ. (b) The constraint function $|\gamma(\mu, \xi, \kappa) - \gamma_t|$.

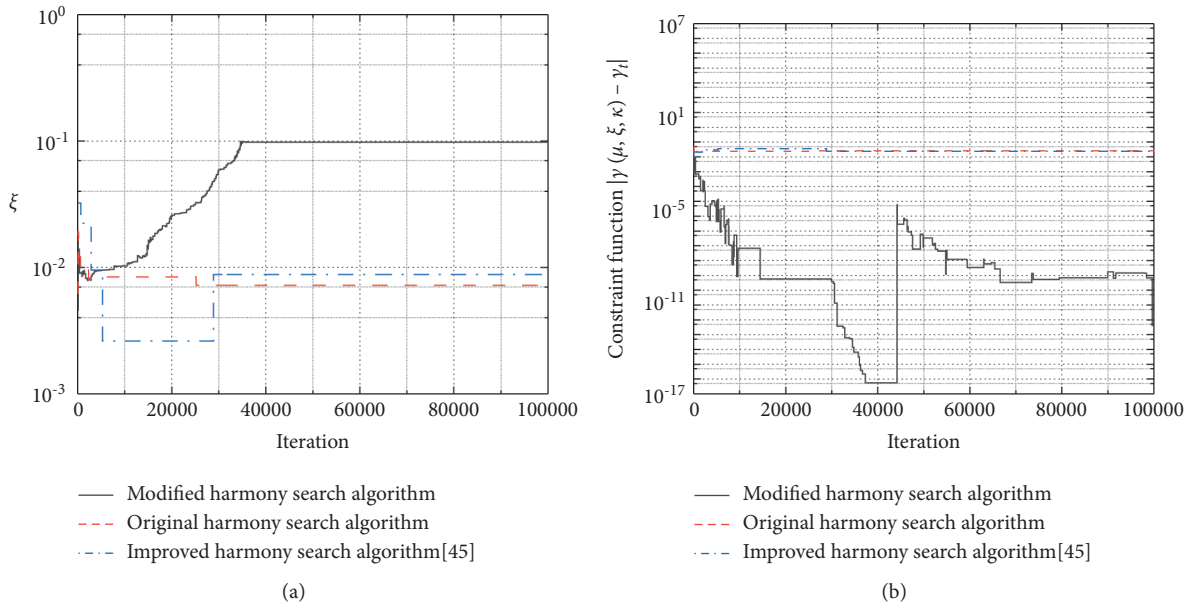

Figure 12: The variation trends of key indices during the optimization process for case 8. (a) The nominal damping ratio ξ. (b) The constraint function $|\gamma(\mu, \xi, \kappa) - \gamma_t|$.

number of successful iterations, that is, the serial number of the iterative step when the new harmony is better than all the harmonies in the *HM*.

Based on the above descriptions, the Python programming language is used to develop an object-oriented computer program termed Modified Harmony Search Algorithm for Optimization of Inerter System (MHSAOIS) to solve the parameter optimization problem of the inerter system.

3.3. Benchmark Test of the Modified Algorithm. Benchmark functions in [50, 54] are selected to make a preliminary test of the performance of the modified

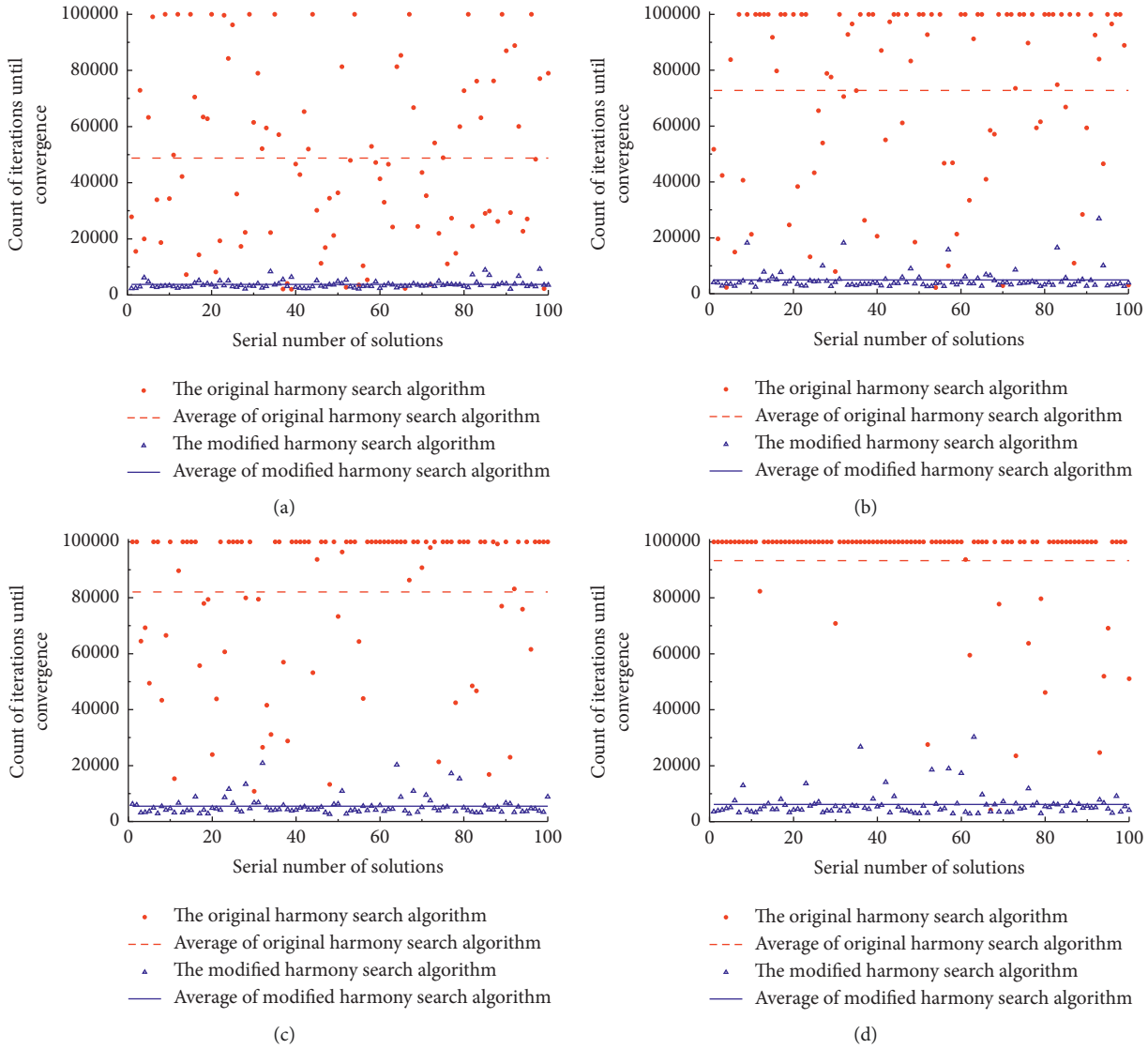

Figure 13: The convergence efficiency of original and modified harmony search algorithms. (a) Relative converge tolerance 20%, (b) relative converge tolerance 10%, (c) relative converge tolerance 5%, and (d) relative converge tolerance 2%.

Table 7: Mean and standard deviation of the count of iterations at convergence for different algorithms.

Relative converge tolerance (%)	Modified harmony search algorithm		Original harmony search algorithm	
	Mean	Standard deviation	Mean	Standard deviation
20	3748.88	1362.16	>48727.18	>31498.65
10	4924.59	3695.10	>72731.49	>32507.04
5	5494.83	3323.34	>82034.17	>26944.20
2	6151.28	4454.48	>93258.13	>18715.29

Note. The symbol ">" indicates that, during the 100 solutions, there are 1 or more nonconvergent solutions.

harmony search algorithm. The benchmark functions are listed in Table 3, where Dim denotes the dimension of the function and $f_{\min}$ denotes the analytical minimum value of the function.

Each benchmark problem is solved 100 times independently by the original, improved [45], and modified harmony search algorithms, and the average values of the benchmark functions are listed in Table 4. It can be found that the values of the benchmark functions solved by the modified and improved algorithms are obviously closer to the analytical solutions than that of the original algorithm. That is, the efficiency of the modified harmony search algorithm is testified.

Table 8: Approximate number of iterations for convergency under different penalty weight strategies.

Case	Fixed penalty weight strategy				Adaptive penalty weight strategy		
	$h = 0.01$	$h = 0.1$	$h = 1$	$h = 10$	$h = h_0 \cdot \delta^{t_s}$	$h = h_0 \sqrt[100]{t}$	$h = h_0 + t/1000$
1	21000	52000	N	N	30000	100000	N
2	N	25000	55000	N	14000	100000	N
3	N	12000	34000	N	8000	80000	N
4	N	N	32500	N	19000	45000	N
5	N	N	N	13000	35000	46000	8500
6	N	N	9000	18000	31000	9000	9000
7	N	N	13500	44000	17000	23000	N
8	N	11000	47000	N	9000	55000	N

Note. N in the table means that the solution does not converge after 100000 iterations.

4. Case Study

4.1. Optimal Design Cases. An SDOF structure is selected and its key parameters are as follows: mass $m = 1900$ ton, stiffness $k = 280000$ kN/m, natural frequency $f = 1.93$ Hz, and period of free vibration $T = 1/f = 0.52$ s. It is planned to equip an inerter system to control its seismic response. Considering the difference in inherent damping ratio ζ and target response mitigation ratio γ_t, 8 design cases are set in Table 5, and the MHSAOIS program is used to solve the optimal design of the key parameters of the inerter system. The parameters of the algorithm are set as $HMS = 50$, $HMCR = 0.9$, $PAR_{\min} = 0.3$, $PAR_{\max} = 0.9$, $bw_{\min} = 0.00001$, and $bw_{\max} = 0.1$.

After optimization, the designed parameters (μ, ξ, and κ) and performance indices (γ and α) are also listed in Table 5. From Table 5, the actual stochastic response mitigation ratio γ based on the modified harmony search algorithm is consistent with the target response mitigation ratio γ_t. The correctness and rationality of the optimized parameters will be verified later.

4.2. Verification of Optimization Objective. To verify the correctness of the obtained parameters, a large number of parameter analyses are carried out for obtaining the values of DDEFs of the inerter system as the parameters change. The results are shown in Figure 4.

In Figure 4, the horizontal and vertical coordinates are the inertance-mass ratio μ and the stiffness ratio κ, respectively, and the height is the DDEF calculated through (16). It can be found that each contour line in the figure is closed and each contour has a single peak value, which is the maximum value of DDEF. The key parameters obtained from the modified harmony search algorithm are marked in the contours, and they are found to be consistent with the peaks of the contours, which verifies that the designed parameters realize the maximization of damping enhancement.

4.3. Efficiency Verification of Modified Harmony Search Algorithm. To investigate the performance and efficiency of the modified harmony search algorithm, the influences of the modified harmony generating strategy and the adaptive penalty weight strategy on the solution efficiency are investigated. Compared with the original harmony search algorithm ($HCR = 0.9$, $PAR = 0.3$, and $bw = 0.01$) and the improved harmony search algorithm [45], the solution efficiency of the modified harmony generating strategy is studied. All design cases in Table 5 are solved 100 times by the original algorithm, the improved algorithm [45], and the modified algorithm, respectively. The maximum number of iterations of each algorithm is set as 100,000. Since the correctness of the optimized parameters in Table 5 is proved by Figure 4, the values of ξ are regarded as the criteria to judge if the solution is converged. That is, if the solved value of ξ is closed (relative error is less than 10^{-2}) to the corresponding value in Table 5, the solution is regarded as converged. The average converged number of iterations and iteration time required for each case are listed in Table 6 (since the improved harmony search algorithm [45] did not converge in all solutions, the results are not listed). It can be seen from Table 6 that the number of iterations and consumed time required by the modified harmony search algorithm are reduced by more than 50% on average

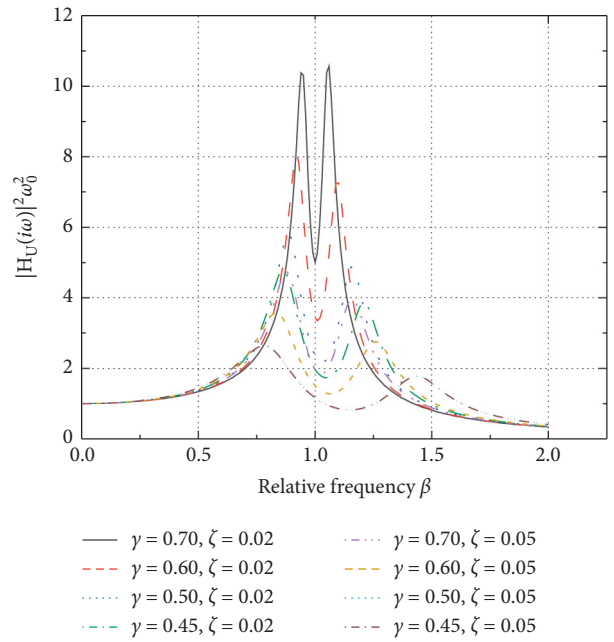

Figure 14: Frequency-domain displacement transfer function curves of SDOF structure with the inerter system.

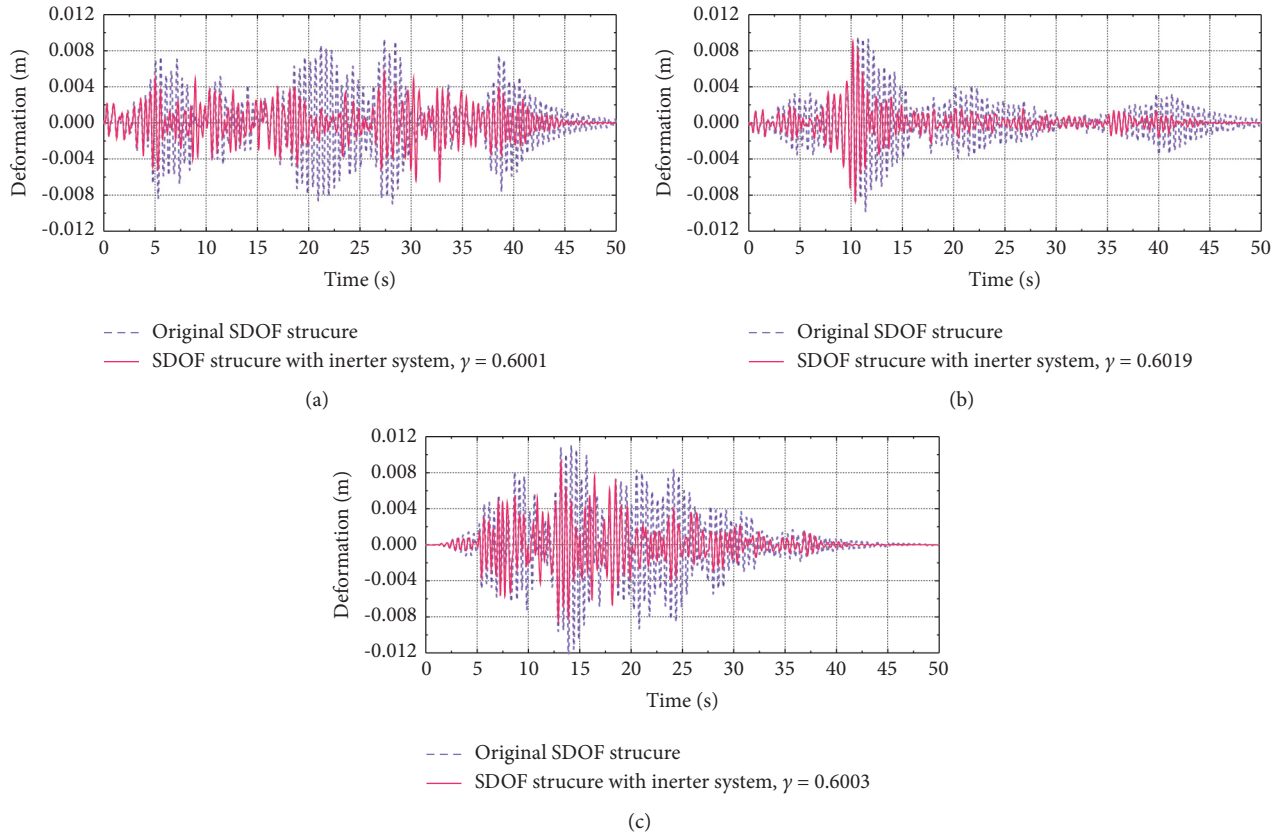

Figure 15: Displacement response curves of structures with inerter systems under different seismic excitations. (a) White noise excitation. (b) Artificial seismic excitation. (c) Natural seismic excitation.

compared with the original harmony search algorithm. Among the design cases, the most obvious solution efficiency enhancement occurs in case 3, and the corresponding number of iterations for convergence and consumed time are reduced by about 90%. This means that the modified algorithm has a stronger solving ability. The variation trends of the nominal damping ratio ξ of the inerter system and the value of the constraint function of each case as the number of iteration increases are shown in Figures 5–12. It can be seen from Figures 5–12 that all the designed cases are converged under the modified harmony search algorithm, but there are nonconvergent cases under the original harmony search algorithm, such as case 1, case 2, case 3, and case 5. As for the improved harmony search algorithm [45], although its performance in the benchmark test (Section 3.3) is the best for unconstrained problems, it failed to converge in all cases here. The variation trends of these nonconvergent cases show that the original harmony search algorithm and the improved harmony search algorithm [45] are easy to fall into a local optimal solution and no longer change during the iteration process. In addition, although the values of the objective functions for case 4, case 6, case 7, and case 8 for both the original algorithm and the improved algorithm [45] are less than that of the modified algorithm, it can be seen that the values of the constraint functions are about 3 orders of magnitude smaller, which means that the constraint conditions are more satisfied. These results prove the advantages of the modified harmony search algorithm over the original one.

Design case 3 is selected to conduct detailed statistical analysis. The problem is solved 100 times independently by the original and modified harmony search algorithms. The value of nominal damping ratio (i.e., the value of the objective function) for design case 3 in Table 5 is used as the criterion for judging convergence, and the tolerances of the relative errors are set as 20%, 10%, 5%, and 2%, respectively, to demonstrate the convergency of the original and modified algorithms. The results are shown in Figure 13 and Table 7. It can be found that the average number of iterations for convergence of the modified algorithm is significantly smaller than that of the original algorithms. As the tolerance decreases, the convergence probability of the original algorithm becomes lower and lower, while the modified algorithm can easily converge after fewer iterations. This proves that the modified harmony search algorithm has a more powerful ability for solving optimization problems.

The next step is to verify the specific advantages of adopting an adaptive penalty weight strategy (equation (28)). The fixed penalty weight strategy and different forms of adaptive penalty weight functions are tested, and the results are shown in Table 8. It can be seen that the fixed penalty weight strategy requires more iterations than the adaptive penalty weight strategy. Furthermore, there are nonconvergent cases under the fixed penalty weight strategy. Meanwhile, it can be seen that the adopted expression of adaptive penalty weight h ($h = h_0 \cdot \delta^{t_s}$,

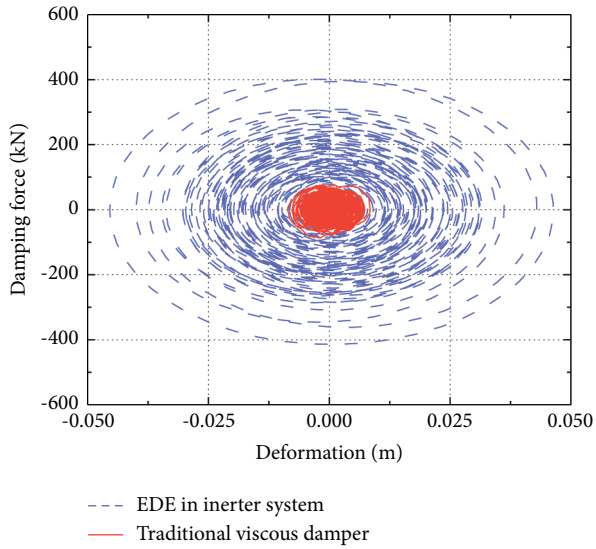

FIGURE 16: Hysteresis curves of a viscous damper within an inerter system and traditional viscous damper (the damping coefficients are identical) under seismic excitation.

i.e., (28)) can give the best solution effect compared with other forms of penalty weight functions because $h = h_0 \cdot \delta^{t_s}$ can guarantee the convergency but the other penalty weight functions cannot. Therefore, the currently adopted adaptive penalty weight strategy is more powerful in solving the optimization problems of inerter systems.

5. Structural Responses in the Frequency Domain and Time Domain

Substituting the parameters in Table 5 into the analytical expression of the displacement response frequency response function ((5)), the frequency-domain displacement transfer function curves are shown in Figure 14. It can be seen that the parameters obtained can effectively control the seismic response of the SDOF structure.

To visually demonstrate the damping enhancement effect, the design parameters of case 2 are chosen as example, and the structure with inerter system and the original structure are analyzed under dynamic excitation. Seismic excitations with different spectral characteristics (white noise excitation, artificial seismic excitation, and natural seismic excitation) are considered, and the displacement responses are shown in Figure 15. It can be found that the displacement response of the structure with the inerter system is smaller than that of the original structure under different seismic excitations, and the root-mean-square response mitigation ratio is similar to the target one ($\gamma_t = 0.6$), which proves the effectiveness of the proposed method and the rationality of design parameters.

In addition, a comparison between the inerter system and the traditional viscous damper is also conducted. An inerter system and a viscous damper (they have the same viscous damping coefficient) are installed in the structure simultaneously. The responses of dampers are shown in Figure 16. The comparison of the hysteresis curves shows that the deformation and damping force of the damper in the inerter system is greater than that of the traditional viscous damper. As for the enclosed area of the hysteresis curve, that is, the dissipated energy, the damper in the inerter system is also significantly larger than the traditional viscous damper.

6. Conclusion

In this paper, a modified harmony search algorithm is proposed to design the inerter system for the maximization of the damping enhancement effect. It is verified that the algorithm is effective and easy to implement, and the following conclusions are drawn:

(1) The key parameters of the inerter system can be effectively obtained according to the target demands by the modified harmony search algorithm. No assumptions or engineering experiences are needed during the optimal design.

(2) The design problem of the maximum damping enhancement of the inerter system can be described as a mathematical optimization problem and the constraint condition can be replaced by a penalty function.

(3) With respect to the original harmony search algorithm, the convergence performance of the modified harmony search algorithm is significantly improved. The number of iterations at the convergence of the modified harmony algorithm can be reduced by 38%~92%, and the consumed time can be reduced by 18% ~ 89%.

(4) This paper only discusses the single-degree-of-freedom structure with the inerter system. The optimization of the multi-degree-of-freedom structure with inerter systems by the modified harmony search algorithm will be further investigated in detail in the future.

Data Availability

The data used to support the findings of this study are included within the article.

Conflicts of Interest

The authors declare that there are no conflicts of interest regarding the publication of this paper.

Acknowledgments

This work was supported by the Foundation of State Key Laboratory of Mechanical Behaviour and System Safety of Traffic Engineering Structures, Shijiazhuang Tiedao University, grant number KF2020-13, and the Project for the Introduction of Overseas Students in Hebei Province (CN), grant number C20190364.

References

[1] J. T. P. Yao, "Concept of structural control," *Journal of the Structural Division*, vol. 98, no. 7, pp. 1567–1574, 1972.

[2] S. Elias and V. Matsagar, "Research developments in vibration control of structures using passive tuned mass dampers," *Annual Reviews in Control*, vol. 44, pp. 129–156, 2017.

[3] I. Takewaki, K. Fujita, K. Yamamoto, and H. Takabatake, "Smart passive damper control for greater building earthquake resilience in sustainable cities," *Sustainable Cities and Society*, vol. 1, pp. 3–15, 2011.

[4] A. Giaralis and F. Petrini, "Wind-induced vibration mitigation in tall buildings using the tuned mass-damper-inerter," *Journal of Structural Engineering*, vol. 143, no. 9, p. 23, 2017.

[5] R. C. Zhang and K. Dai, "Response control of wind turbines with ungrounded tuned mass inerter system (TMIS) under wind loads," *Wind and Structures*, vol. 32, pp. 573–586, 2021.

[6] K. Ikago, K. Saito, and N. Inoue, "Seismic control of single-degree-of-freedom structure using tuned viscous mass damper," *Earthquake Engineering & Structural Dynamics*, vol. 41, no. 3, pp. 453–474, 2012.

[7] E. Barredo, A. Blanco, J. Colín et al., "Closed-form solutions for the optimal design of inerter-based dynamic vibration absorbers," *International Journal of Mechanical Sciences*, vol. 144, pp. 41–53, 2018.

[8] T. Arakaki, H. Kuroda, F. Arima, Y. Inoue, and K. Baba, "Development of seismic devices applied to ball screw : Part 1 Basic performance test of RD-series," *AIJ Journal of Technology and Design*, vol. 5, no. 8, pp. 239–244, 1999.

[9] P. Brzeski, M. Lazarek, and P. Perlikowski, "Experimental study of the novel tuned mass damper with inerter which enables changes of inertance," *Journal of Sound and Vibration*, vol. 404, pp. 47–57, 2017.

[10] F. C. Wang, M. F. Hong, and T. C. Lin, "Designing and testing a hydraulic inerter," *Proceedings - Institution of Mechanical Engineers, Part C: Journal of Mechanical Engineering Science 1989-1996*, vol. 225, no. 1, pp. 66–72, 2010.

[11] A. Gonzalez-Buelga, L. R. Clare, S. A. Neild, S. G. Burrow, and D. J. Inman, "An electromagnetic vibration absorber with harvesting and tuning capabilities," *Structural Control and Health Monitoring*, vol. 22, no. 11, pp. 1359–1372, 2015.

[12] A. Gonzalez-Buelga, L. R. Clare, S. A. Neild, J. Z. Jiang, and D. J. Inman, "An electromagnetic inerter-based vibration suppression device," *Smart Materials and Structures*, vol. 24, no. 5, p. 055015, 2015.

[13] Y. Hu, M. Z. Chen, Z. Shu, and L. Huang, "Analysis and optimisation for inerter-based isolators via fixed-point theory and algebraic solution," *Journal of Sound and Vibration*, vol. 346, pp. 17–36, 2015.

[14] S. Krenk and J. HøGsberg, "Tuned resonant mass or inerter-based absorbers: unified calibration with quasi-dynamic flexibility and inertia correction," *Proceedings of the Royal Society A: Mathematical, Physical & Engineering Sciences*, vol. 472, no. 2185, p. 20150718, 2016.

[15] I. F. Lazar, S. A. Neild, and D. J. Wagg, "Using an inerter-based device for structural vibration suppression," *Earthquake Engineering & Structural Dynamics*, vol. 43, no. 8, pp. 1129–1147, 2014.

[16] A. Gonzalez-Buelga, I. F. Lazar, J. Z. Jiang, S. A. Neild, and D. J. Inman, "Assessing the effect of nonlinearities on the performance of a tuned inerter damper," *Structural Control and Health Monitoring*, vol. 24, no. 3, p. e1879, 2017.

[17] D. De Domenico, N. Impollonia, and G. Ricciardi, "Soil-dependent optimum design of a new passive vibration control system combining seismic base isolation with tuned inerter damper," *Soil Dynamics and Earthquake Engineering*, vol. 105, pp. 37–53, 2018.

[18] D. D. Domenico and G. Ricciardi, "Improving the dynamic performance of base-isolated structures via tuned mass damper and inerter devices: a comparative study," *Structural Control and Health Monitoring*, vol. 25, pp. 2231–2224, 2018.

[19] L. Marian and A. Giaralis, "Optimal design of a novel tuned mass-damper–inerter (TMDI) passive vibration control configuration for stochastically support-excited structural systems," *Probabilistic Engineering Mechanics*, vol. 38, pp. 156–164, 2014.

[20] D. Pietrosanti, M. D. Angelis, and M. Basili, *Optimal Design and Performance Evaluation of Systems with Tuned Mass Damper Inerter (TMDI)*, Earthquake Engineering & Structural Dynamics, 2017.

[21] G. Park, A. Giaralis, and L. Marian, "SPIE proceedings [SPIE SPIE smart structures and materials + nondestructive evaluation and health monitoring - las vegas, Nevada, United States (sunday 20 march 2016)] active and passive smart structures and integrated systems 2016 - use of inerter devices," *International Society for Optics and Photonics*, vol. 9799, p. 97991G, 2016.

[22] D. De Domenico and G. Ricciardi, "An enhanced base isolation system equipped with optimal tuned mass damper inerter (TMDI)," *Earthquake Engineering & Structural Dynamics*, vol. 47, no. 5, pp. 1169–1192, 2018.

[23] X. Jin, M. Z. Q. Chen, and Z. Huang, "Minimization of the beam response using inerter-based passive vibration control configurations," *International Journal of Mechanical Sciences*, vol. 119, pp. 80–87, 2016.

[24] L. Zhang, S. Xue, R. Zhang, L. Xie, and L. Hao, "Simplified multimode control of seismic response of high-rise chimneys using distributed tuned mass inerter systems (TMIS)," *Engineering Structures*, vol. 228, p. 111550, 2021.

[25] R. Faraj, J. Holnicki-Szulc, L. Knap, and J. Senko, "Adaptive inertial shock-absorber," *Smart Materials and Structures*, vol. 25, no. 3, p. 035031, 2016.

[26] A. Javidialesaadi and N. E. Wierschem, "An inerter-enhanced nonlinear energy sink," *Mechanical Systems and Signal Processing*, vol. 129, pp. 449–454, 2019.

[27] Z. Zhao, Q. Chen, R. Zhang, C. Pan, and Y. Jiang, "Energy dissipation mechanism of inerter systems," *International Journal of Mechanical Sciences*, vol. 184, p. 105845, 2020.

[28] Q. Z. Chen and R. Zhang, "An inerter-system chain and energy-based optimal control of adjacent single-degree-of-freedom structures," *Smart Structures and Systems*, vol. 28, pp. 245–259, 2021.

[29] C. Pan and R. Zhang, "Design of structure with inerter system based on stochastic response mitigation ratio," *Structural Control and Health Monitoring*, vol. 25, no. 6, p. e2169, 2018.

[30] C. Pan, R. Zhang, H. Luo, C. Li, and H. Shen, "Demand-based optimal design of oscillator with parallel-layout viscous inerter damper," *Structural Control and Health Monitoring*, vol. 25, no. 1, p. e2051, 2018.

[31] R. Z. Zhang, L. Zhang, C. Pan, D. De Domenico, and Q. Chen, "Targeted modal response control of structures using inerter systems based on master oscillator principle," *International Journal of Mechanical Sciences*, vol. 206, p. 106636, 2021.

[32] R. Zhang, Z. Zhao, C. Pan, K. Ikago, and S. Xue, "Damping enhancement principle of inerter system," *Structural Control and Health Monitoring*, vol. 27, no. 5, p. 889, 2020.

[33] C. Pan, J. Jiang, R. Zhang, and Y. Xia, "Closed-form design formulae for seismically isolated structure with a damping

enhanced inerter system," *Structural Control and Health Monitoring*, vol. 28, no. 12, p. 43353, 2021.

[34] R. Zhang, J. Jiang, Y. Jia, and C. Wang, "Influence of mechanical layout of shape memory alloy damping inerter (SDI) systems for vibration control," *Smart Materials and Structures*, vol. 30, no. 8, p. 085021, 2021.

[35] J. G. Fang, G. Y. Sun, N. Qiu, N. H. Kim, and Q. Li, "On design optimization for structural crashworthiness and its state of the art," *Structural and Multidisciplinary Optimization*, vol. 55, no. 3, pp. 1091–1119, 2017.

[36] A. H. Gandomi, X. S. Yang, and A. H. Alavi, "Cuckoo search algorithm: a metaheuristic approach to solve structural optimization problems," *Engineering with Computers*, vol. 29, no. 1, pp. 17–35, 2013.

[37] A. Giaralis and A. A. Taflanidis, "Optimal tuned mass-damper-inerter (TMDI) design for seismically excited MDOF structures with model uncertainties based on reliability criteria," *Structural Control and Health Monitoring*, vol. 25, no. 2, p. e2082, 2018.

[38] X. S. Yang and S. Deb, "Multiobjective cuckoo search for design optimization," *Computers & Operations Research*, vol. 40, no. 6, pp. 1616–1624, 2013.

[39] A. R. Yildiz, "Comparison of evolutionary-based optimization algorithms for structural design optimization," *Engineering Applications of Artificial Intelligence*, vol. 26, no. 1, pp. 327–333, 2013.

[40] S. Mirjalili, S. M. Mirjalili, and A. Lewis, "Grey wolf optimizer," *Advances in Engineering Software*, vol. 69, pp. 46–61, 2014.

[41] S. Talatahari and M. Azizi, "Optimization of constrained mathematical and engineering design problems using chaos game optimization," *Computers & Industrial Engineering*, vol. 145, p. 106560, 2020.

[42] L. Abualigah, D. Yousri, M. Abd Elaziz, A. A. Ewees, M. A. Al-qaness, and A. H. Gandomi, "Aquila Optimizer: a novel meta-heuristic optimization algorithm," *Computers & Industrial Engineering*, vol. 157, p. 107250, 2021.

[43] M. Azizi, "Atomic orbital search: a novel metaheuristic algorithm," *Applied Mathematical Modelling*, vol. 93, pp. 657–683, 2021.

[44] G. Bekdaş and S. M. Nigdeli, "Estimating optimum parameters of tuned mass dampers using harmony search," *Engineering Structures*, vol. 33, no. 9, pp. 2716–2723, 2011.

[45] H. Yazdi, H. Saberi, H. Saberi, and F. Hatami, "Designing optimal tuned mass dampers using improved harmony search algorithm," *Advances in Structural Engineering*, vol. 19, no. 10, pp. 1620–1636, 2016.

[46] S. M. G. Nigdeli and C. Alhan, *Optimization of Seismic Isolation Systems via harmony Search. Engineering Optimization*, Engineering Optimization, 2013.

[47] A. Ocak, G. Bekda, and S. M. Nigdeli, *A Metaheuristic-Based Optimum Tuning Approach for Tuned Liquid Dampers for Structures*, The Structural Design of Tall and Special Buildings, 2021.

[48] S. Ulusoy, G. Bekdas, S. M. Nigdeli, S. Kim, and Z. W. Geem, "Performance of optimum tuned PID controller with different feedback strategies on active-controlled structures," *Applied Sciences*, vol. 11, no. 4, p. 1682, 2021.

[49] S. H. Crandall and W. D. Mark, *Random Vibration in Mechanical Systems*, Academic Pr, 1963.

[50] ZW. Geem, J. H. Kim, and G. V. Loganathan, "A new heuristic optimization algorithm," *harmony search. Simulation*, vol. 76, pp. 60–68, 2001.

[51] M. G. Omran and M. Mahdavi, "Global-best harmony search," *Applied Mathematics and Computation*, vol. 198, no. 2, pp. 643–656, 2008.

[52] M. Fesanghary, M. Mahdavi, M. Minary-Jolandan, and Y. Alizadeh, "Hybridizing harmony search algorithm with sequential quadratic programming for engineering optimization problems," *Computer Methods in Applied Mechanics and Engineering*, vol. 197, no. 33-40, pp. 3080–3091, 2008.

[53] M. Mahdavi, M. Fesanghary, and E. Damangir, "An improved harmony search algorithm for solving optimization problems," *Applied Mathematics and Computation*, vol. 188, no. 2, pp. 1567–1579, 2007.

[54] X. Yao, Y. Liu, and G. Lin, "Evolutionary programming made faster," *IEEE Transactions on Evolutionary Computation*, vol. 3, no. 2, pp. 82–102, 1999.